Diffused-Quantum-Well Vertical Cavity Fabry-Perot Reflection Modulator

Wallace C.H. Choy, S.F. Ip and E. Herbert Li

Department of Electrical and Electronic Engineering, The University of Hong Kong, Pokfulam Road, Hong Kong

***Abstract* - This is a first report to use diffused quantum well (DFQW) as the active cavity of the Fabry-Perot reflection modulator. Apart from the simple fabrication process of the DFQW, this material system provides a wavelength tuning range and improves the modulation properties of the device which thus is competitive to the same kind of modulator.**

I. INTRODUCTION

Currently, surface-normal Fabry-Perot (FP) etalon modulators based on III-V multiple quantum well (MQW) semiconductors for potential applications such as two-dimensional arrays for interconnection, and optical processing have gained considerable interest. This type of modulator has the advantage of providing a large area in the coupling of light in and out of the device and is compatible with vertical opto-electronic integrating technology [1]. Moreover, this structure of modulator provides long effective optical interaction path and thus reduces the applied voltage swing [2]. In this work, annealing induced non-square diffused-QW (DFQW) structure[3] is first introduced as the intrinsic material in the asymmetric-FP vertical cavity so that the operation wavelength λ_{op} of the modulator can be fine tuned by controlling the disordering of regular as-growth QW. This structure can serve as a high performance FP modulator by improving the modulation properties and providing an operation wavelength tuning range. It is expected that this DFQWs based FP modulator will become an important candidate for the vertical integrating technology. The electro-optical effects of DFQW structure on the total reflectance R_{tot} of the modulator are analyzed together with the figures of merit, change of R_{tot}, (ΔR_{tot}), and the ratio $\Delta R_{tot}/R_{tot}$.

II. MODELING

We consider the DFQW resonant-etalon reflection modulator structure in a simple way, as shown in Fig. 1(a), where the inner intrinsic DFQW consists of 61 periods of 101Å/100Å $Al_{0.3}Ga_{0.7}As/GaAs$. The extent of diffusion is characterized by a diffusion length L_d ($L_d = 0$ represents the as-growth QW) [3]. The front and back quarter wavelength Bragg reflectors are alternative AlAs and AlGaAs layers with reflective indices taken from [4] which are p- and n- doped as in a p-i-n structure. The bottom reflectance R_B is set at about 0.97, the top one R_T is calculated from the relation $R_T = R_b\exp(-2\alpha_c l_c)$ where l_c and α_c are the cavity length and absorption coefficient respectively, α_c is calculated from a model similar to [5] without the polarization sensitivity; the relation of R_T is the impedance-matching condition for zero total reflectivity at resonance[2] so that the contract ratio CR of the modulation can become infinity. The reflectance of the FP modulator can be calculated by using the scattering matrices method as shown in Fig. 1b. The arrow indicates the direction of propagation of the field, where F (forward) and B (backward) are the electric field of the light. The total reflectance is defined as $R_{tot} =(B_1/F_1)^2= |(s_{21} + R_{B5}^{1/2} s_{22})/(s_{11} - R_{1T}^{1/2}s_{12})|^2$, where R_{B5} and R_{1T} are the reflectance of the interface between (B, 5) and between (1, T) respectively, the negative sign of R_{1T} indicates that the refractive index of medium T is higher than that of medium 1 since medium 1 is considered to be air ($n_{air}=1$), and s_{ij} are the matrix elements of a 2×2 scattering matrix S. S is defined as $M_T \times M_{QW} \times M_B$, where M_j *is the scattering matrix of region j for* $F_j= m_{j11}F_{j+1} + m_{j12}B_{j+1}$ and $B_j= m_{j21}F_{j+1} + m_{j22}B_{j+1}$, m_{jab} are elements of M_j, and the subscripts a and b are integer 1 or 2. It is assumed that the field in top and bottom reflectors (medium T and B) will only undergo phase change without any residence loss while the field in the intrinsic DFQW layer will involve both phase changes $\exp(i\delta_c l_c)$ and loss $\exp(-\alpha_c l_c)$. The phase change per unit length is defined as $\delta_i=2\pi n_i/\lambda_{op}$ where n_i and λ_{op}, are the refractive index of medium (i) and the operational wavelength, respectively.

III. RESULTS

It is interesting to note that the FP modulator can operate at FP mode for cases from L_d 0 to 40 Å stepped by 10Å without any re-design of the active region of the modulator. However, since the operation wavelength will shift while the QW structure undergoes an interdiffusion,

0-7803-2624-5/95/$4.00

the top and bottom Bragg reflectors, the number of the alternative layers, and the thickness of each quarter wavelength layer have to be rearranged. The number of period of top and bottom reflectors are 8.5 and 16.5 of alternative 734Å (AlAs) and 639Å ($Al_{0.3}Ga_{0.7}As$) respectively when the cavity structure is as-growth square wells (L_d= 0). While the QW structure undergoes an interdiffusion to L_d = 40Å , the top and bottom reflectors will be amended to 7.5 and 16.5 periods of alternative 633 Å (AlAs) and 548Å ($Al_{0.3}Ga_{0.7}$ As) respectively. As a whole , the total thickness of the modulator will be reduced for different DFQW's cavities. Table 1 shows the modulation properties of the DFQWs modulators with an identical thickness of cavity. For the cases from L_d = 0 to 20Å, the change of reflectance (ΔR_{tot}) have roughly same value. Moreover, there are two possible λ_{op} that the first λ_{op} of L_d = 10 will have relative low residence loss but high minimum value of R_{tot}, R_{tot} (min), at FP mode while the second λ_{op} is just vice versa. The R_{tot} (min) for the case L_d = 30Å is the lowest (1.0418×10^{-5}) with low residence loss. Although the ΔR_{tot} is also reduced to minimum (0.100) when comparing with other L_ds' cases, the figure of the merit $\Delta R_{tot}/R_{tot}$ is extremely high about 9600. If the interdiffusion is further increased to L_d = 40Å , the λ_{op} will further blue-shift [6] to 0.7645μm. Also the applied electric field F (kV/cm) will reduce to 50 - 80 kV/cm though the R_{tot}(min) become high. All in all, the same as-growth QW cavity structure can operate between 0.8747 and 0.794μm under different interdiffusion from L_d=0 to 30Å. If high R_{tot}(min) is not an obstacle in an operation, the wavelength tuning range will increase to (0.8747 to 0.7645μm) about 110nm.

In fact, the whole modulation will further improve by adjusting the cavity thickness l_c for $n\pi$ phase variation of the field in different L_ds' cases. In order to compare with the result of as-growth square QW modulator, the adjusted l_c of different L_ds' cases is set nearest to the l_c of the square QW modulator. Fig.2a and Fig.2b show the reflectance spectra of different applied field of the cases L_d =0 (square QW) and L_d = 40Å respectively. For the case L_d =0, the OFF-state operated at λ_{op} = 0.875μm with field F=130kV/cm while the On-state is with field F=0. It is found that the λ_{op} of FP mode of higher field operation will shift to shorter wavelength because the change of reflective index Δn of the DFQW cavity under reverse bias. The Δn is due to the Quantum Confined Stark Effect and can be calculated from the spectrum of the change of absorption coefficient by Kramer-Krönig relation. Moreover, for the spectra of the case F=0, 50 and 90 kV/cm, the reflectance are close together at the λ_{op}. This can be explained by the packing of absorption spectra at the λ_{op} as shown in [7]. The R_T is designed for zero R_{tot} at F= 130kV/cm (OFF-state), so from figure 2, the modulation is operated at the ON-OFF state with $\Delta R_{tot}/R_{tot}$ = 0.6427/ 3.313×10^{-3} = 194. In Fig.2b, the case of L_d = 40Å, the λ_{op} is blue shift to 0.7727μm. The FP resonance with zero reflectance is operated at F=80kV/cm, the ΔR_{tot} of ON(F=0) and OFF(F=80kV/cm) states is 0.6872 with extremely low R_{tot}(min) value 4.7633×10^{-5} . Thus the $\Delta R_{tot}/R_{tot}$ is as high as 15000. This value is the highest from what we recognize in the published. Moreover, the applied field required for operation also reduces from 130kV/cm at L_d =0 to 80kV/cm in this case. This can therefore minimize the voltage swing. The results of other applied field are shown in Table 2. The ΔR_{tot} increases from L_d = 0 to L_d = 20Å and then reduce to 0.4873 at L_d = 40Å. While the R_{tot}(min) keeps very low and only within an acceptable fluctuation, the residence loss of different L_ds' cases is just between 550 and 860 cm^{-1} except the second possible λ_{op} which can operate at low R_{tot}(min), of L_d = 10Å with residence loss 1200cm^{-1}. Two outstanding cases L_d = 30 and 40Å are mentioned that for the case L_d = 30Å, the residence loss reduces to lowest as well as low R_{tot} (min), 350 cm^{-1} and 2.327×10^{-4} respectively. While for the case L_d = 40Å, the applied field can be reduced to 80 kV/cm (lower power consumption) with extremely high $\Delta R_{tot}/R_{tot}$ 15000 as mentioned above. Together with the distinct feature of blue shift of λ_{op} and simple thermal annealing processes for producing DFQW, this FP reflection modulator will become competitive in same kind of modulator.

IV. CONCLUSION

In conclusion, we have analyzed the reflectivity property of a vertical cavity FP reflection modulator with different L_d's and its electro-optical effect. The blue shift of λ_{op} is due to the effect of DFQW which suggests a wide band-width FP reflection modulator with $\Delta\lambda_{op} \cong$ 110nm. Moreover, the L_d = 30Å DFQW modulator with adjusted l_c can operate at lowest residence loss and low R_{tot} (min) implies highest figure of merit $\Delta R_{tot}/R_{tot}$ while the case L_d = 40Å , only 80 /130× 100%= 61% applied field is required and achieved highest $\Delta R_{tot}/R_{tot}$= 15000. All these properties make the DFQWs vertical cavity modulator become competitive device.

ACKNOWLEDGMENT

This work is financially supported by the HKU-CRCG grant.

REFERENCE

[1] G.A. Evan, et al., " Characteristics of Coherent Two-Dimensional Grating Surface Emitting Diode Laser Arrays During CW Operation", IEEE J. of Quantum Electron. vol. 27, pp.1594-1605, 1991.

[2] K.K. Law, J.L. Merz, and L.A. Golden, "Superlattice Surface-Normal Asymmetric Fabry-Perot Reflection Modulators: Optical Modulation and Switching", J. of Quantum Electron. vol. 29, pp.727-739, 1993.

[3] E.H. Li, B.L. Weiss and K.S. Chan, "Effect of interdiffusion in the subbands in an $Al_xGa_{1-x}As/GaAs$ single-quantum-well structure", Phys. Rev. B, vol. 46, no.23, pp.15181-15192, 1993.

[4] B. Jensen and W. D. Jensen, "The Reflective Index Near the Fundamental Absorption Edge in $Al_xGa_{1-x}As$ Ternary Compound Semiconductors", IEEE J. of Quantum Electron. vol. 27, pp.40-44, 1991.

[5] E.H. Li, K.S. Chan, B.L. Weiss, and J. Micallef, "Quantum-confined Stark effect in interdiffused AlGaAs/GaAs quantum well", Appl. Phys. Lett. vol. 63, pp.533-535, 1993.

[6] E.H. Li and W.C.H. Choy, " Electro-optical and Electro-absorptive Modulation Properties in Interdiffusion Modified AlGaAs/GaAs Quantum Wells", IEEE Photon. Technol. Lett. to be published.

[7] W.C.H. Choy and E.H. Li, IEEE, "High performance Diffused Quantum Wells Fabry Perot reflection modulator", J. of Quantum Electron., submitted for published.

L_d(Å)	λ_{op}(μm)	ΔR_{tot}	R_{tot}(min)	F(kV/cm) [ON-STATE]	F(kV/cm) [OFF-STATE]	α_{loss}(cm^{-1})
0	0.8747	0.6427	3.3125×10^{-3}	0	130	550
10	0.8564	0.6615	0.1628	0	130	860
10	0.8522	0.6482	0.0892	0	130	1200
20	0.8202	0.6899	0.00346	130	90	1090
30	0.7940	0.1000	1.0418×10^{-5}	110	90	640
40	0.7645	0.3150	0.585	80	50	1050

Table 1. Features of the DFQW reflection modulators with an identical thickness of cavity.

L_d(Å)	λ_{op}(μm)	ΔR_{tot}	R_{tot}(min)	F(kV/cm) [ON-STATE]	F(kV/cm) [OFF-STATE]	l_c(μm)	α_{loss} (cm^{-1})
0	0.8747	0.6427	3.313×10^{-3}	0	130	1.2273	550
10	0.8564	0.7059	3.789×10^{-2}	0	130	1.2063	860
10	0.8523	0.6300	6.694×10^{-3}	0	110	1.2063	1200
20	0.8270	0.6612	2.050×10^{-3}	0	130	1.2817	738
30	0.7991	0.5766	2.327×10^{-4}	0	110	1.2399	350
40	0.7713	0.6872	4.763×10^{-5}	0	80	1.2844	691

Table 2. Features of the DFQW reflection modulators with l_c nearest to that of the square QW modulator.

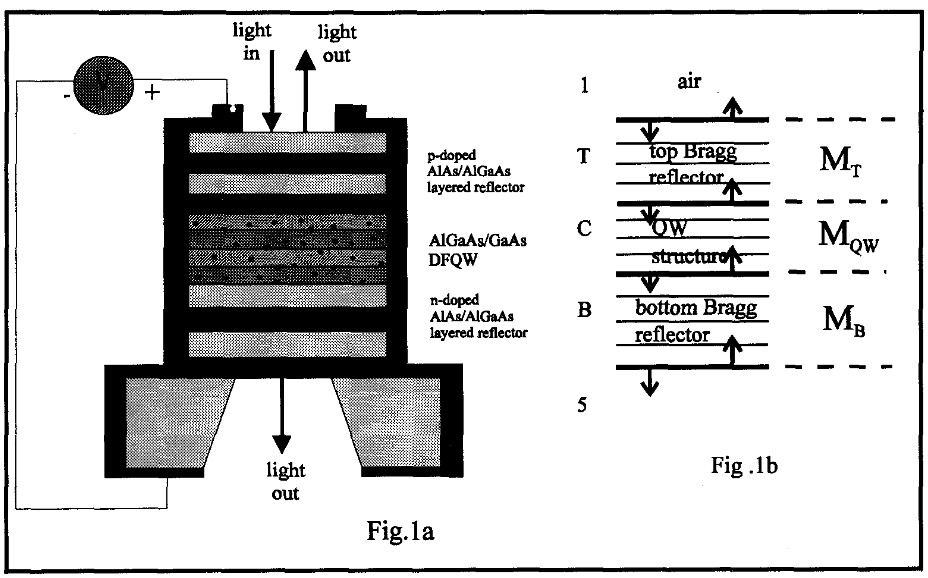

Fig. 1a Schematic cross-section of the three-sections exptiaxial Febry-Perot reflection modulator
Fig. 1b Illustration of the scattering matrices in deriving design equations.

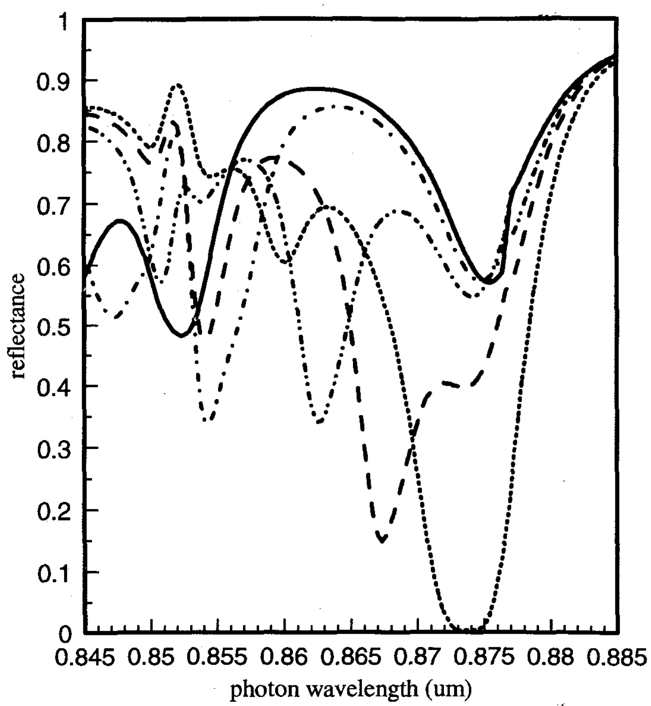

Fig.2a The reflectance spectra of Ld=0 with field F=0 (soild), 50 (dash-dot), 90 (dash-double dot,), 110 (long-dash) and130 kV/cm (dot).

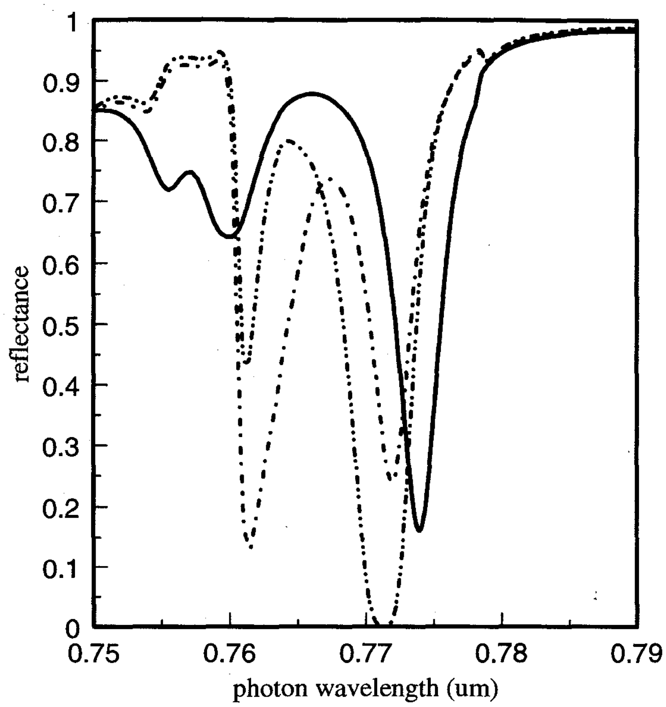

Fig.2b The reflectance spectra of Ld=40 A with field F=0 (soild), 50 (dash-dot), 80 (dash-double dot).